Gamow-Teller and First-Forbidden Transition Strengths in Astrophysical Processes

Toshio Suzuki[1,2], Takashi Yoshida[3], Michio Honma[4], Hélène Mao[1,5], Takaharu Otsuka[6,7] and Toshitaka Kajino[3,8]

[1]Department of Physics, College of Humanities and Sciences, and Graduate School of Integrated Basic Sciences, Nihon University, Sakurajosui-3-25-40, Setagaya-ku, Tokyo 156-8550, Japan
[2]Center for Nuclear Study, University of Tokyo, Hirosawa, Wako-shi, Saitama, 351-0198, Japan
[3]Department of Astronomy, Graduate School of Science, University of Tokyo, Hongo, Bunkyo-ku, Tokyo 113-0033, Japan
[4]Center for Mathematical Sciences, University of Aizu, Aizu-Wakamatsu, Fukushima 965-8580, Japan
[5]ENSPS, Pôle API -Parc d'Innovation, Boulevard Sébastien Brant, BP 10413, 67412 ILLKIRCH CEDEXL, France
[6]Department of Physics and Center for Nuclear Study, University of Tokyo, Hongo, Bunkyo-ku, Tokyo 113-0033, Japan
[7]RIKEN, Hirosawa, Wako-shi, Saitama 351-0198, Japan
[8]National Astronomical Observatory of Japan, Mitaka, Tokyo 181-8588, Japan

E-mail: suzuki@chs.nihon-u.ac.jp

Abstract. Gamow-Teller (GT) and first-forbidden (FF) transitions in nuclei and their possible consequences on astrophysical processes in stars are discussed. GT transition strengths in fp-shell nuclei are studied by shell model calculations with the use of new shell model Hamiltonians, GXPF1. Neutrino-nucleus reaction cross sections are re-evaluated and compared with previous investigations. Proton emission cross sections on ^{56}Ni are pointed out to be enhanced and lead to the enhancement of the production yields of ^{55}Mn and ^{59}Co in population III supernovae. Next, electron capture reactions on Ni and Fe isotopes in steller environments are studied. The capture rates depend sensitively on the distributions of the GT strengths. Capture rates on ^{58}Ni and ^{60}Ni obtained by GXPF1 are found to reproduce rather well those obtained from experimental GT strengths. Finally, beta decays of the N=126 isotones are studied by shell model calculations taking into account both the GT and FF transitions. The FF transitions are found to be important to reduce the half-lives by twice to several times of those by the GT contributions only. Possible implications on the short half-lives of the waiting point nuclei on the r-process nucleosynthesis are discussed for certain astrophysical conditions.

1. Introduction

Spin dependent transitions in nuclei are investigated based on recent advances in shell model calculations, and applied to astrophysical processes. In sect, 2, new GT transition strengths are obtained for Ni isotopes by using GXPF1 Hamiltonian for fp-shell [1], and neutrino-nucleus reaction cross sections for supernova neutrinos and electron capture reaction rates in stellar environments are re-evaluated. In sect. 3, beta decay half-lives of N=126 isotones are obtained

by including both the GT and FF transition contributions. Possible consequences of the short half-lives on the r-process nucleosynthesis are discussed.

2. Neutrino-Nucleus and Electron Capture Reactions in Ni Isotopes

2.1. Gamow-Teller Strengths

Recent new shell model Hamiltonians for fp-shell, GXPF1 [1] and KB3G [2], can describe spin properties of nuclei very well. In particular, GXPF1J [1] reproduces well the GT strength distribution in ^{58}Ni as well as the magnetic dipole strength distributions in fp-shell nuclei such as ^{48}Ca, ^{50}Ti, ^{52}Cr and ^{54}Fe [1]. The observed values of the sum of the GT strength in Ni and Fe isotopes are also rather well reproduced by both the Hamiltonians as shown in Fig. 1. The distributions of the GT strengths by GXPF1J are generally more fragmented compared with those by KB3G, and the strengths remain up to higher excitation energies. This can be seen from the larger averaged energies of the GT sum for GXPF1J compared to KB3G as shown in Fig. 2. We here apply these developments and achievements obtained by recent progress in shell model studies of stable and unstable nuclei to astrophysical processes in stars.

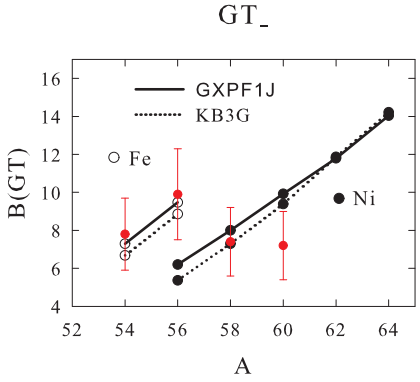

Figure 1. Sum of the GT strength, $B(GT)$, for Fe and Ni isotopes. Calculated values obtained by GXPF1J and KB3G as well as experimental values [3] are shown.

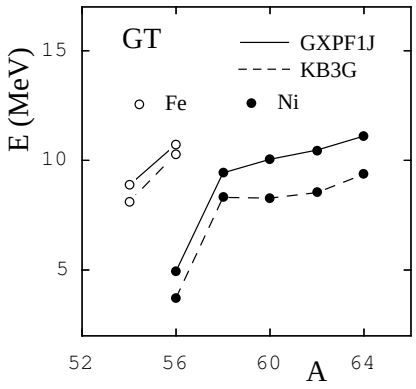

Figure 2. Averaged energies of the GT strength distributions obtained by GXPF1J and KB3G for Fe and Ni isotopes.

2.2. Neutrino-Nucleus Reactions induced by Supernova Neutrinos and Synthesis of Mn

Here, we discuss neutral current reactions on ^{56}Ni induced by supernova neutrinos. The branching ratio for proton emission channel becomes large due to the large spreading of the GT strength in ^{56}Ni by GXPF1J [4]. The cross section for the proton emission channel is larger than that for the γ emission channel for GXPF1J. The proton emission cross section thus gets larger for GXPF1J than the case for KB3G and previous calculations [5].

This leads to the enhancement of the production rate of Mn in supernova explosions [4]. The Mn element can be produced through the reaction chain; ^{56}Ni (ν, ν'p) ^{55}Co (e^-, ν) ^{55}Fe (e^-, ν) ^{55}Mn. The amount of ^{55}Mn produced in a $15M_\odot$ population III supernova is enhanced for GXPF1J compared to the standard value by ref. [5] (see ref. [4] for the details). This shows the importance of the role of the ν-process in supernova explosions on nucleosynthesis.

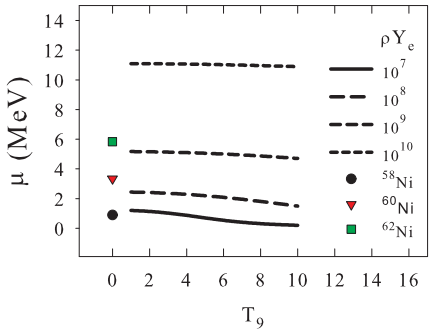

Figure 3. Chemical potentials of electrons in high densities and temperatures. Threshold energies of the electrons for the capture reactions on Ni isotopes are denoted by symbols.

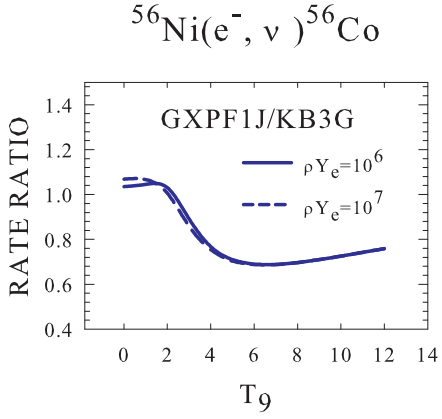

Figure 4. Ratios of the capture rates by GXPF1J over those by KB3G.

2.3. Electron Capture Rates in Steller Environments

We discuss electron capture rates on Ni isotopes in steller environments, that is, for high densities $\rho = 10^7 \sim 10^{10}$ mol/cm^3 and high temperatures $T = 10^9 \sim 10^{10}$ K. Chemical potential of electrons become larger in these environments as shown in Fig. 3. Calculated rates for ^{56}Ni (e^-, ν) ^{56}Co are obtained by GXPF1J as well as KB3G. The universal quenching of g_A^{eff}/g_A =0.74 is adopted for the calculations of the capture rates. The ratios of the rates by GXPF1J over KB3G are shown in Fig. 4. The ratios are reduced by about 30% from 1 at T_9 >3 ($T_9 = T/10^9$) as the transitions to higher excited states get hindered for GXPF1J due to the more spreading in the GT strength.

Calculated capture rates for ^{58}Ni (e^-, ν) ^{58}Co obtained by GXPF1J are shown in Fig. 5 as well as the rate obtained by using the experimental GT strength [6]. The GT strength distribution obtained by GXPF1J is found to be rather consistent with the observed GT strength (see Fig. 5). The shell model capture rates by GXPF1J reproduces well the experimental capture rate as shown in Fig. 6. This is also true for the capture rates for ^{60}Ni (e^-, ν) ^{60}Co. The rates obtained by experimental GT strength [7] (see Fig. 7) are extremely well reproduced by shell model calculations with GXPF1J as shown in Fig. 8.

The present more accurate capture rates by GXPF1J lead to an important step toward better evaluations of lepton-to-baryon ratio in collapsing iron cores to become proto-neutron stars and the productioin yields of elements in supernovae.

3. Beta Decays of N=126 Isotones

3.1. Half-Lives of the Isotones with GT and FF Transitions

Beta decays of N=126 isotones, the waiting point nuclei for the r-process, are studied by shell model calculations. Both the Gamow-Teller (GT) and first-forbidden (FF) transitions are taken into account to evaluate the half-lives of the nuclei (Z = 64-72). A shell model interaction, modified from G-matrix elements, that reproduces well the observed energy levels of the isotones with a few (2 to 5) proton holes outside ^{208}Pb [8] is used.

The GT strengths obtained by the shell model calculations for nuclei with Z=64 and 72

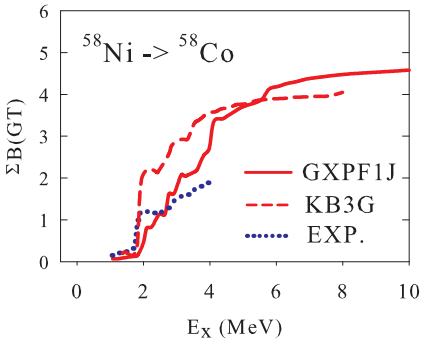

Figure 5. Sum of the GT_+ strength in ^{58}Ni up to the excitation energy of the daughter nucleus, E_x. Calculated values for GXPF1J and KB3G as well as the experimental values are shown.

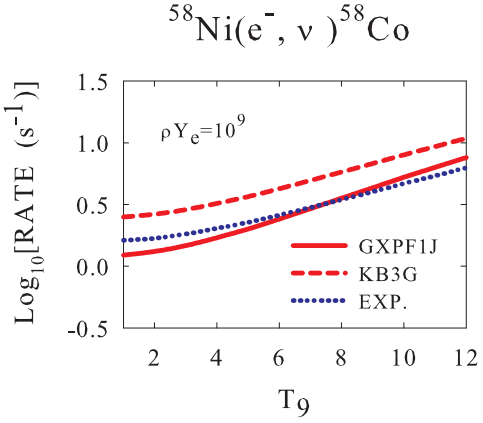

Figure 6. Calculated capture rates for ^{58}Ni obtained by GXPF1J and KB3G are compared with that evaluated for the experimental $B(GT)$ values.

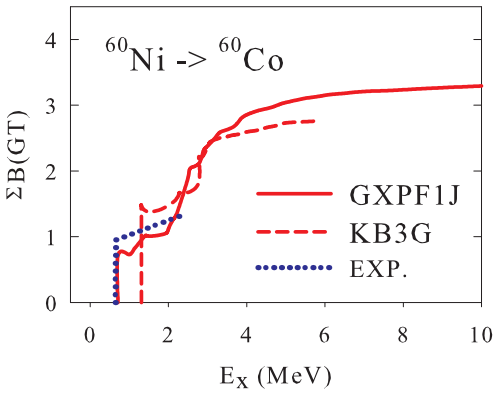

Figure 7. The same as in Fig. 5 for ^{60}Ni.

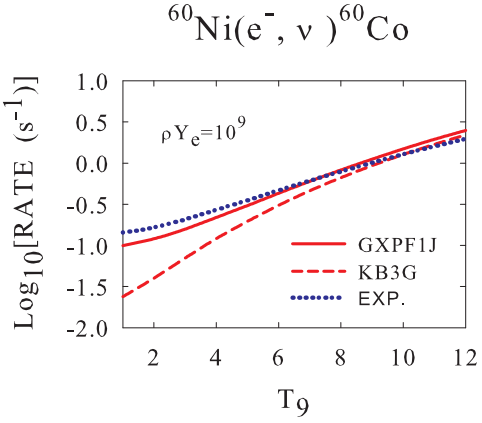

Figure 8. The same as in Fig. 6 for ^{60}Ni.

are shown in Figs.9 and 10, respectively. The magnitude of the strength as well as the energy difference between the energies of the parent nucleus and the GT states are larger for nuclei with more proton holes. The calculated spin-dipole strengths for 1^- are also shown in Figs. 11 and 12 for Z=64 and 72, respectively. Similar situation as in the GT case is seen.

Decay rates for the FF transitions are evaluated [9] by including the quenching of the axial vector coupling constant. A quenching of g_A^{eff}/g_A^{free}=0.7 is taken for both the GT and FF transitions. Calculated half-lives obtained by the GT contributions are found to be consistent with those in [10]. The half-lives become shorter for smaller Z isotones as both the strength and the energy difference between initial and final states get larger. The FF transitions are found to be important to reduce the half-lives by twice to several times of those given by the GT contributions only. Short half-lives of the isotones obtained are shown in Fig.13.

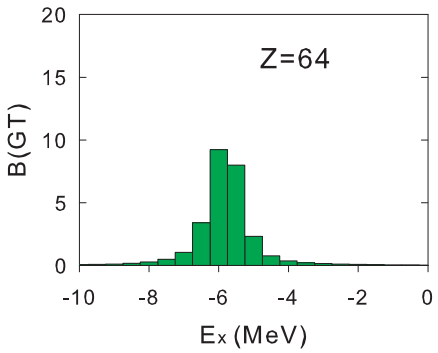

Figure 9. Calculated GT strengths for the N=126 isotones with Z=64 by shell model calculations. E_x =0 denotes the energy of the parent state.

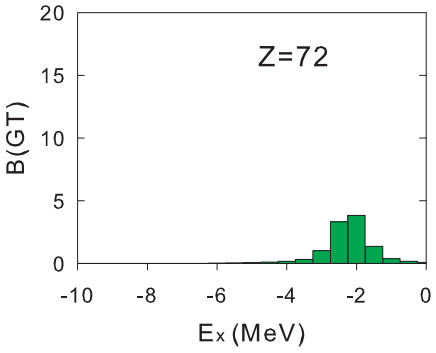

Figure 10. Calculated GT strengths for the N=126 isotones with Z=72 by shell model calculations.

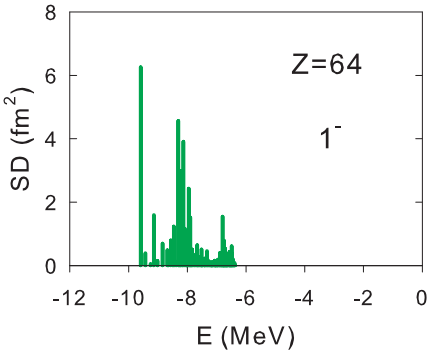

Figure 11. Calculated spin dipole strengths (1^-) for the N=126 isotones with Z=64.

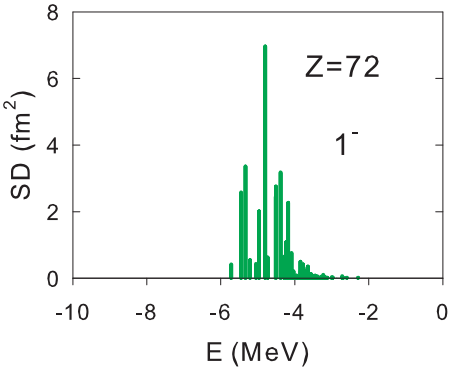

Figure 12. Calculated spin dipole strengths (1^-) for the N=126 isotones with Z=72.

3.2. Effects on the Third Peak of the r-Process Nucleosynthesis

We discuss possible effects of the short half-lives of the waiting point (WP) nuclei at N=126 obtained here on the r-process nucleosynthesis. The dependence of the abundances of the elements around mass number A∼190 on the half-lives of the nuclei are investigated for various astrophysical conditions. We show one example of the effects on the nucleosynthesis during supernova explosions in Fig. 14. Constant entropy wind model is used for the explosion. The temperature is assumed to decrease from $T_{9,i} = 9$ to $T_{9,f} = 1$ by $T_9 = (T_{9,i} - T_{9,f}) \exp(-t/\tau) + T_{9,f}$ with τ =0.1s, and the entropy per baryon of the wind corresponds to S/k =400. The initial electron to baryon ratio is taken to be 0.40. The r-process network consists of 3517 species of nuclei. The abundance of the elements obtained by using the present short half-lives in the network are compared with those obtained with the use of the standard data of ref. [11]. We find a slight shift of the third peak of the element abundances toward higher mass region.

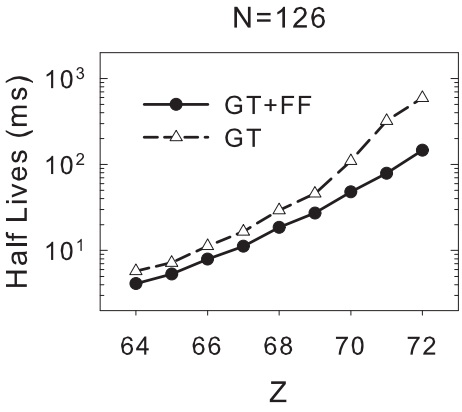

Figure 13. Calculated half-lives of the N=126 isotones by the shell model calculations. Results obtained by the GT contributions as well as those including both the GT and FF contributions are shown.

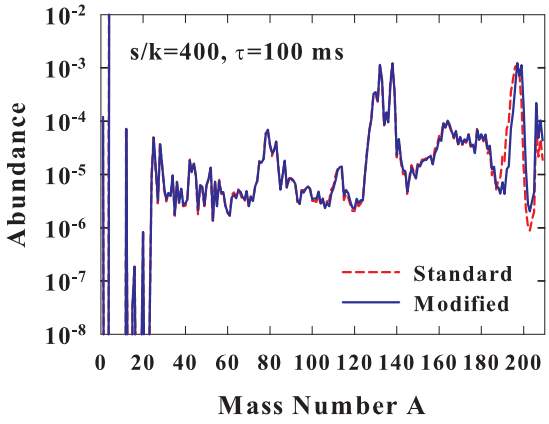

Figure 14. The r-process abundance distributions obtained by using the present short half-lives (solid line) and the standard half-lives (dashed line).

Due to the shorter half-lives of the WP nuclei, the r-process proceeds more rapidly and the WP isotones with higher Z accumulate more at the freezing time of the neutron flow. The successive β-decays naturally lead to larger abundances of the elements at higher mass region. The present shift of the third peak toward higher mass region is a robust effect which should be taken into account in addition to various nuclear inputs such as mass formulae and neutron capture cross sections that can affect the third peak region. The magnitude of the shift of the peak is of similar order as that caused by the use of different mass formulae [11]. When the decrease of the temperature becomes slower or the entropy of the system is larger, the magnitude of the shift of the peak gets larger. It is important to include the robust effects to find out if the explosive supernova explosion is really the site for the r-process.

Acknowledgements: This work has been supported in part by Grant-in-Aid for Scientific Research (C) 22540290, MEXT, Japan.

References

[1] Honma M, Otsuka T, Brown B. A., and Mizusaki T 2002 *Phys. Rev.* C **65** 061301(R); 2005 **69** 034335; Honma M et al., 2005 *J. Phys. Conf. Ser.* **20** 7
[2] Caurier E, Martínez-Pinedo G, Nowacki, Poves A and Zuker P 2005 *Rev. Mod. Phys.* **77** 427
[3] J. Rapaport et al. 2005 *Nucl. Phys.* **A410** 371
[4] Suzuki T, Honma M, Higashiyama K, Yoshida T, Kajino T, Otsuka T, Umeda H and Nomoto K 2009 *Phys. Rev.* C **79** 061603(R)
[5] Woosley S. E., Hartmann D. H., Hoffman R. D. and Haxton W. C. 1990 *Astrophys. J.* **356** 272
[6] Hagemann et al. 2004 *Phys. Lett.* **B579** 251
[7] N. Anantaraman et al. 2008 *Phys. Rev.* C **78** 065803
[8] Steer S. J. et al. 2008 *Phys. Rev.* C **78**, 061302; Rydström L et al. 1990 *Nucl. Phys.* **A512** 217
[9] Warburton E. K., Becker J. A., Brown B. A. and Millener D. J. 1998 *Annals of Physics* **187** 471
[10] Langanke K and Martínez-Pinedo G 2003 *Rev. Mod. Phys.* **75** 819
[11] Möller P, Pfeiffer B and Kratz K.-L. 2003 *Phys. Rev.* C **67** 055802; Möller P, Nix J. R. and Kratz K.-L. 1997 *At. Data and Nucl. Data Tables* **66** 131